Effect of different TM modes on the sensitivity of surface plasmon resonance based optical fiber sensor

SAXENA PRAGYA[*], PRADEEP TEOTIA, R. S. KALER
Thapar University, Patiala, India

The purpose of this paper is to analyse the SPR based optical fiber sensor (core diameter ≈ 6um) on which a layer of gold metal having thickness (h_{Au} ≈ 0.5-5 nm) is deposited by removing cladding for particular sensing region. We have examined the effect of different mode profiles (TM_{01}, TM_{02}, TM_{03}….TM_{08}) on the guiding region for different thicknesses of metal layer. The various mode profiles are further investigated to examine the impact on the sensitivity of said sensor. The said mode profiles for above said sensor are studied using finite difference time domain (FDTD) simulations. Transmission spectra for different TM modes are also compared with respect to the operating wavelength. We observed that the thickness of metal film and operating wavelength are responsible for variation in the sensitivity with respect to TM modes of the said sensor.

1. Introduction

Numerous techniques have been used for sensing, such as doppler effect, interferometry, photolumnisense and surface plasmon resonance (SPR). Apart from all other sensing techniques, SPR is emerged as a powerful detection technique in real time with variety of diverse applications such as life science, electrochemistry, chemical vapour detection, food and environmental safety and beyond. In SPR, the desired quantity is determined by measuring the refractive index (RI), absorbance and fluorescence properties of measured parameter [1]. In this technique, when the p-polarised light with propagation constant equal to that of surface plasmon wave (an electromagnetic wave supported by metal-dielectric interface) is incident on metal-dielectric interface, a strong absorption of light takes place, hence SPR causes a reduction in the intensity of light reflected at specific angle or wavelength from the glass side of the sensor surface [2].

Masaru Mitsushio et al. [3] investigated the response curves and sensor properties of Al-deposited optical fibers with Al film thicknesses of 7–70 nm based on surface plasmon resonance (SPR). S. Lee et al. [4] presented the method for determining the effective indices, field distributions and mode numbers of the guiding modes for planar waveguides. Ruschin et al. [5] and Lit et al. [6] both used simplified equations that were transformed from the field- transfer matrix to characterize the mode properties for planer waveguides. Above said study limits the mode profile only to certain parameters. None of them discussed the sensitivity and mode relations. Thereby we describe, for the first time to our knowledge, the effect of different mode profiles (TM_{01}, TM_{02}, TM_{03}, ….. TM_{08}) on the guiding region for different thicknesses of metal layer. The different mode profiles are further investigated to examine the impact on the sensitivity of said sensor.

This paper is divided in four sections. In section 2, the simulation setup for comparison of sensor performance with varying parameters, is discussed with component details. Section 3 deals with the detailed discussion of results observed after the simulation. Section 4 gives the conclusion of the dependence of sensor performance with varying parameters.

2. Simulation setup

The SPR sensing is based on principle of (ATR) attenuated total reflection with Kretschmann's configuration [7]. In this paper the SPR based fiber optic sensor is presented with fiber core-Au-sensing medium as shown in Fig. 1. As structure follows, cladding is firstly removed over the core (numerical aperture = 0.18 and fiber core diameter = 6 μm) to firm up sensing region which is coated with thin metal layer and further this portion is covered with sensing medium. The light from the broadband source is launched into one end of the fiber with proper optics and the transmitted light is detected at the other end of the optical fiber.
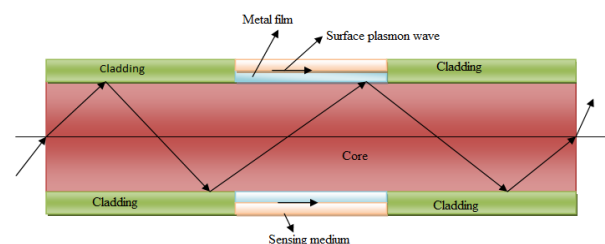
Fig. 1. Schematic diagram of an SPR based optical fiber sensor

Table 1. Parameters used for optical fiber

Parameter	Numerical value
Fiber core diameter,D	6 μm
Numerical aperture (NA)	0.18
Sensing region length,L	100 μm

In Fig. 1, the fiber core is considered as first layer. The refractive index of fused silica (n_1) varies with wavelength according to Sellmeier dispersion relation given as [8]:

$$n_1(\lambda) = \sqrt{1 + \frac{A_1\ \lambda^2}{\lambda^2 - B_1^2} + \frac{A_2\ \lambda^2}{\lambda^2 - B_2^2} + \frac{A_3\ \lambda^2}{\lambda^2 - B_3^2}} \qquad (1)$$

Where λ = wavelength of incident light in μm with sellmeier coefficients A_1 =0.6961663, A_2 = 0.4079426, A_3 =0.8974794, B_1=0.0684043 μm, B_2= 0.1162414 μm, B_3= 9.896161 μm, with λ=1.55 μm, n_1 (λ) comes out to be 1.4440.

Second layer is made up of Au metal and the dielectric constant of any metal can be written according to Drude model [9] as,

$$\epsilon_m\ (\lambda) = \epsilon_{mr} + i\ \epsilon_{mi} = 1 - \frac{\lambda^2 \lambda_c}{\lambda_p^2(\lambda_c + i\lambda)} \qquad (2)$$

Where λ_p= 1.6826 ×10⁻⁷m (plasma wavelength) and λ_c= 8.9342×10⁻⁶m (collision wavelength)

The Au metal layer is surrounded with sensing medium, with dielectric constant ε_s ,which is related to refractive index of sensing medium n_s, as $\varepsilon_s = n_s^2$

The resonance condition for excitation of surface plasmon wave is [10]:

$$\frac{2\pi}{\lambda} n_1 \sin\theta = Re\ \{K_{sp}\} \qquad (3)$$

where $K_{sp} = \frac{w}{c}\sqrt{\frac{\epsilon_m \epsilon_s}{\epsilon_m + \epsilon_s}}$ is propagation constant of the surface plasmon, ω is frequency of incident light and c is speed of light in vacuum. By observing the shift in the resonance wavelength, a change in the refractive index of sensing medium can be measured.

When the wave equations are solved by using cylindrical co-ordinate system, it gives the radial variation of electric and magnetic field distribution. Inside the core, field distribution is oscillatory in nature, which is represented by Bessel functions and inside cladding, field is monotonically decaying in nature, which is represented by modified Bessel functions. Due to field distribution in core and cladding, the propagation constant β can be written in bounded form like [11],

$$\beta_2 < \beta\ < \beta_1 \qquad ; \text{ where } \beta_1 \text{ and } \beta_2 \text{ are phase constants of the material of core and cladding respectively.}$$

$\beta_0\, n_2 < \ \beta\ < \beta_0\, n_1$; where β_0 is phase constant of wave in vacuum.

$n_2 < \beta\ /\ \beta_0 < n_1$ or we can write as

$$n_2 < n_{eff} < n_1 \qquad (4)$$

Where n_{eff} is effective modal index and n_1 and n_2 are refractive index of core and cladding of fiber respectively. By considering n_{eff}, transverse magnetics (TM) modes can be calculated.

3. Result and discussion

In the previous sections, we discussed various components used in the simulation setup. Using this setup the measurement of magnitude of dip in transmittance curve for different cases has been performed. The result discussed below gives the comparison of transmittance curves for all the considered cases.

In SPR based fiber optic sensor, TM modes are calculated by considering the effective modal index, they can be designated as: TM_{0m}= $TM_{01,}$ $TM_{02.........}$. Mode patterns are related to the variation of light intensity across the plane perpendicular to the direction of propagation and have certain properties such as, the electric field varies across the guiding region; evanescent field which is generated due to surface plasmon resonance decreases exponentially outside the core. Fig.2 as shown below describes that 'm' gives the number of zero crossings performed by electric field which is penetrated through guiding region. Low order modes exist which are nearly parallel to the boundary at a given thickness of gold layer h_{Au}, while higher order modes have steep zigzag paths. Higher order modes penetrate deeply into cladding and have much more losses.

The above described properties can easily be seen in the Fig. 2 showing all the 9 TM modes, which are calculated by considering the metal thickness (d_m) of around 0.5 at operating wavelength (λ) 1.55 μm in SPR based fiber optic sensor.

In FDTD simulation, with given thicknesses and effective index of core and cladding, 9 TM modes have been observed with different effective modal indices and which are responsible for the variation of intensity in sensing curve with varying modes and it is being shown that all TM modes can be excited at one observation point i.e., at same resonance wavelength for the given incident angle. However, all TM modes respond to different modal indices, so there is a variation in the magnitude of the dip. The above described properties can easily be seen in the Fig. 3 as shown below.
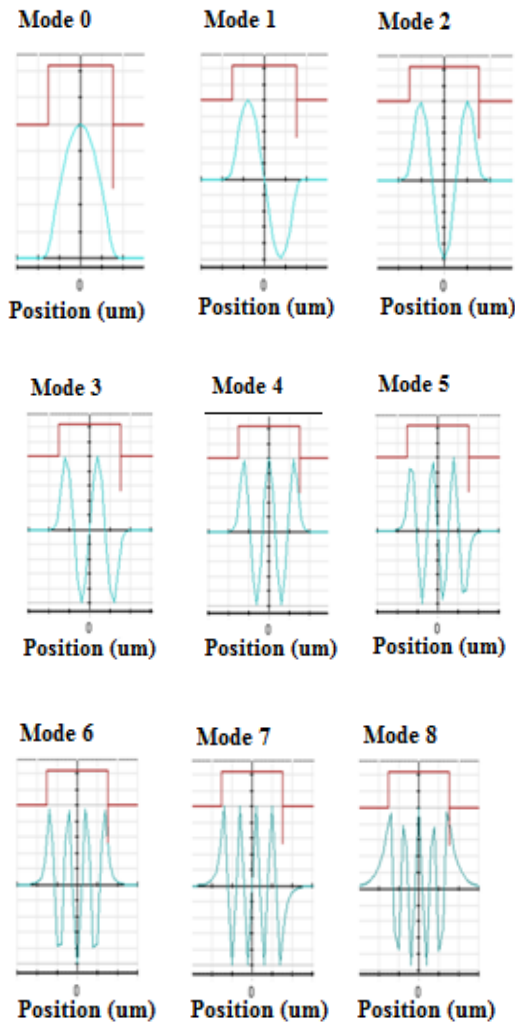
Fig. 2. Different TM modes generated in SPR based fiber optic sensor
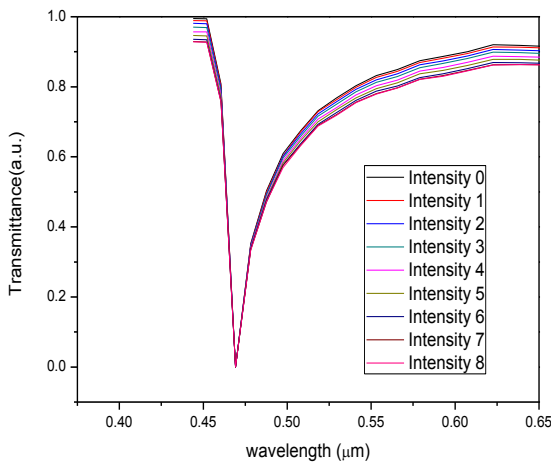
Fig. 3. Variation of Intensity in transmittance curve with all TM modes

The variation of intensities for all 9 TM modes with respect to the sensitivity are shown in Fig. 3. These are calculated by considering the metal thickness (d_m) of around 0.5 nm at operating wavelength (λ) 1.55 µm in SPR based fiber optic sensor.
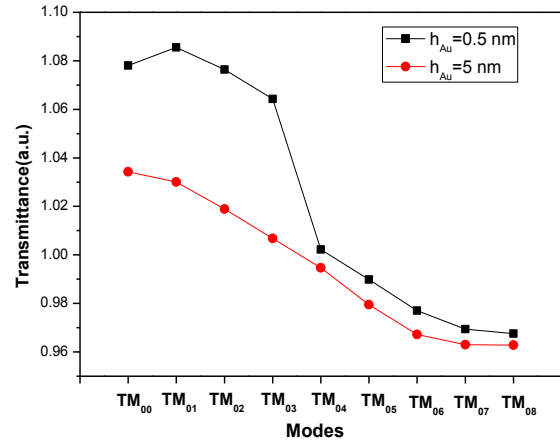
Fig. 4. Shift in the intensity of transmittance curve for different thicknesses of metal film

The effect of modes on the SPR-based fiber optic sensor has been studied with some consideration of thickness of metal layer and operating wavelength. For these generated modes, it has kept in mind that below this thickness of metal layer h_{Au}, all above said modes will not prevail. We compare the result of transmission spectrum for all 9 TM modes, for metal layer having thickness ($h_{Au} \approx 0.5\text{-}5$ nm), as shown in Fig. 4. Further by increasing the thickness of metal film, we analysed 9 TM modes but with different effective modal indices from the optimised thickness of metal film ($h_{Au=}$ 0.5 nm) and which are also responsible for the variation of intensity in sensing curve with varying TM modes. Fig. 4 also depicts that when we increase the thickness of metal film, the variation in intensity is less than that obtained at optimised thickness.
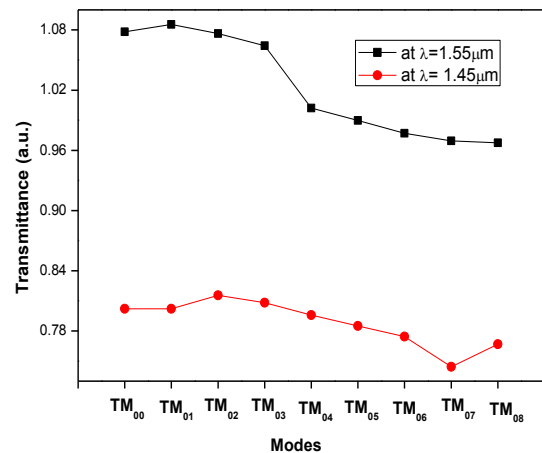
Fig. 5. Shift in the intensity of transmittance curve f or different operating wavelengths

The intensities for all TM modes with respect to the sensitivity for varying operating wavelengths (1.55 µm - 1.45 µm) have been compared and shown in Fig. 5 and it also illustrates that, by decreasing the operating wavelength, still we observed all TM modes but with different effective modal indices from those observed at wavelength of 1.55 µm and which are also responsible for the variation of intensity in sensing curve with varying TM modes.
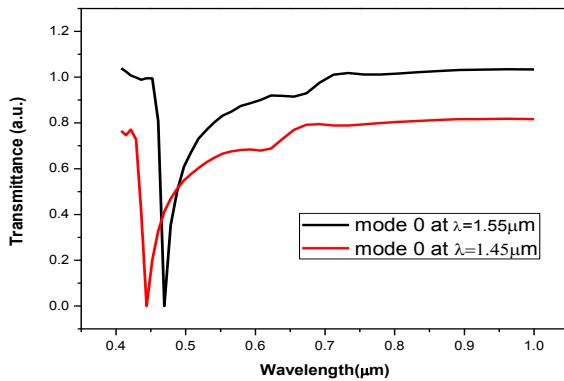
Fig. 6. Shift in resonance wavelength of sensing curve for gold

Fig. 6 is describing that at operating wavelength 1.55 µm, the resonance wavelength is equal to 0.4691 µm whereas at operating wavelength 1.45 µm the resonance wavelength is 0.4439 µm. So there is shift of 0.0252 µm in resonance wavelength with different operating wavelengths. This case explains that when we are changing the operating wavelength with the given configuration, there is shift in the resonance wavelength with the variation in the magnitude of the dip in transmittance curve with varying modal index.

4. Conclusion

The concept of modes for transmittance curve in SPR for different configurations has been presented. The various mode profiles are further investigated to examine the impact on the sensitivity of said sensor. All mode profiles for this sensor are studied using finite difference time domain simulations. Transmission spectra for different TM modes, are also compared for different operating wavelengths. We observed that the thickness of metal film and operating wavelength are responsible for variation in the transmittance with respect to TM modes of the said sensor.

References

[1] J. Homola, S. Y. Sinclair, G. Gauglitz, Sensors and Actuators B, **54**(1), 13 (1999).
[2] B. Gupta, R. Verma, Hindawai Publishing Corporation, Journal of Sensors, 1 (2009).
[3] M. Mitsushioa, K. Watanabeb, Y. Abeb, M. Higoa, Sensors and Actuators A: Physical, **163**(1), 1 (2010).
[4] S. Lee, K. Kim, Journal of the Korean Physical Society, **51**(1), 104 (2007).
[5] G. Griffel, S. Ruschin, N. Croitoru, J. Opt. Soc. Am. A., **4**, 1296 (1987).
[6] J. W. Y. Lit, Y.-F. Li, D. W. Hewak, Canadian Journal of Physics, **66**(10), 914 (1988).
[7] E. Kretschmann, H. Reather, Zeitschrift für Naturforschung, **23A**, 2135 (1968).
[8] A. Ghatak, K. Thyagarajan, UK: Cambridge University Press, 1999.
[9] M. Ordal, L. Long, R. Bell, S. Bell, R. Bell, R. A. Jr., C. Ward, Applied Optics, **22**, 1099 (1983).
[10] A. K. Sharma, R. Jha B. Gupta, IEEE Sensors Journal, **7**(8), 1118 (2007).
[11] H. Kogelnik, Springer Berlin Heidelberg, 7 (1988).

_____
*Corresponding author: pragyamitra@gmail.com